

# BEHAVIOR OF INFLATABLE DAMS UNDER HYDROSTATIC CONDITIONS

Abdullah Ali Nasser Alhamati<sup>1</sup>, Thamer Ahmed Mohammed<sup>2\*</sup>, Jamalodin Norzaie<sup>2</sup>, Abdul Halim Ghazali<sup>2</sup> and Karim Khalaf Al-Jumaily<sup>3</sup>

Received: Sept 1, 2004; Revised: Nov 18, 2004; Accepted: Mar 8, 2005

## Abstract

Inflatable dams are flexible cylindrical inflatable and deflatable structures made of rubberized material attached to a rigid base and inflated by air, water, or a combination of air/water. The interest in inflatable dams is increasing because of the ease of placement and construction. In this study the behavior of air or water-inflated dams is physically and theoretically analyzed under different conditions of internal pressure, upstream and downstream water depth. Experimental data obtained on a laboratory test facility for air-inflated and water-inflated dams were presented and compared with the theoretical results estimated from a developed computer program describing height, cross-sectional profiles and cross-sectional areas of the dams. Good agreement was obtained between the theoretical and experimental results. Further theoretical analyses were conducted to investigate the behavior of the dams under different conditions.

**Keywords:** Inflatable dam, hydrostatic pressure, internal pressure, dam shape, tension

## Introduction

In order to control the flow of water in rivers, streams and canals, it is essential to construct hydraulic structures. Some of these structures are used to control water level. An example of a structure used to control the water level is the inflatable dam. An inflatable dam is a simple and portable barrier made of a flexible membrane, which is filled with air or water or both, and fixed to a canal bed. This type of structure is considered as more economical compared with the rigid types of control structures constructed from concrete, masonry, and steel (Imbertson,

1960; Anwar, 1967; Binnie *et al.*, 1973; Alwan, 1979; Al-shami, 1983; Dumont, 1989; Takasaki, 1989; Tam, 1998; Zhang *et al.*, 2002).

Anwar (1967); Harrison (1970, 1971); Parbery (1976, 1978); Alwan (1979); Al-shami (1983); Nicholas and Rangaswami (1983) and Abd alsaber (1997); presented several mathematical models to analyze the inflatable dam.

Plaut and Fagan (1988); Plaut and Leeuwrik (1988) and Hsieh *et al.* (1989) studied the effects of the weight of the dam

---

<sup>1</sup> University of Thamar, Department of Dams Engineering, Thamar, Yemen

<sup>2</sup> University Putra Malaysia, Department of Civil Engineering, Faculty of Engineering, Selangor, Malaysia, E-mail: thamer@eng.upm.edu.my

<sup>3</sup> University of Technology, Department of Building & Construction Engineering, Baghdad, Iraq

\* Corresponding author

membrane on the vibration of the inflatable dams.

In this study, the effects of the internal pressure, upstream water head and inflating medium (air and water) under hydrostatic conditions on the behavior of the inflatable dams were studied. The theoretical study is based on the work of Harrison (1970) and a computer program was developed to conduct the theoretical analysis.

### Basic Equations and Theoretical Analysis

Analysis of the inflatable dam involves the determination of tension in the dam material and predicting the cross-sectional of the dam. Several investigators analyzed it under hydrostatic and hydrodynamic conditions, by using different methods in order to predict dam profiles. However, the methods used are complicated and required a number of assumptions for inflatable dam boundary conditions. The assumed boundary conditions may be far from actual dam behavior at site.

The analysis carried out by Harrison (1970) depends on three basic assumptions and these assumptions are:

- i) The behavior of the three-dimensional structure could be represented reasonably by the behavior of a two-dimensional transverse section of unit width.
- ii) The perimeter of the cross-section of the dam is composed of a finite number of small straight elements, the static loads acting on each element length caused by water and air

pressures could be considered acting as concentrated loads at the nodes each of such element.

- iii) The material of the dam is elastic and that the stress-strain relationship of the material can be assumed to be linear.

However, in this study, the following modifications to Harrison's assumption were made:

- i) The static loads due to water and air pressures are acting on the elements.
- ii) Non-linear stress-strain relationship for the dam material is considered in the analysis.

The present study adapted the theoretical analysis developed by Harrison (1970) to predict the cross-section of inflatable dams under hydrostatic conditions and a computer program has been developed using visual basic. The analysis predicts the tension along the membrane and the cross-section of the inflatable dam.

### Forces Acting on the Membrane of the Dam

The forces acting on the dam under the hydrostatic conditions are:

- i) Internal air or water pressure.
- ii) upstream water pressure.
- iii) Downstream water pressure.
- iv) Weight of the dam material.

These forces acting on air-inflated and water-inflated dam are shown in Figure 1(a) and (b).

The total length of the membrane of the dam is divided into (n) elements while the resulting nodes from this division are (n+1) (Figure 2). The forces acting on each element

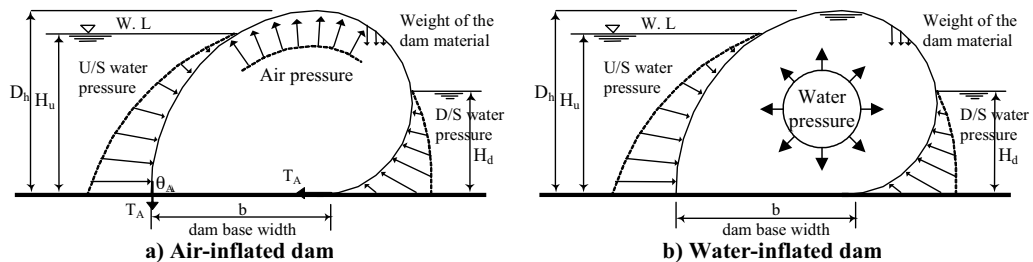


Figure 1. Forces acting on the dam (Hydrostatic condition)

are dependent on the location of the particular element within the dam profile; some elements receive upstream hydrostatic force (upstream element). Other elements receive only downstream hydrostatic force (downstream element) while all the elements receive internal pressure. The forces are transmitted from one element to the adjacent element and progressively, the analysis continuing to the last element.

The forces acting on an upstream element and downstream element of a dam per unit length are shown in Figure 3. It should be noted that when the forces acting on the element their effects will transfer to the nodes of such element

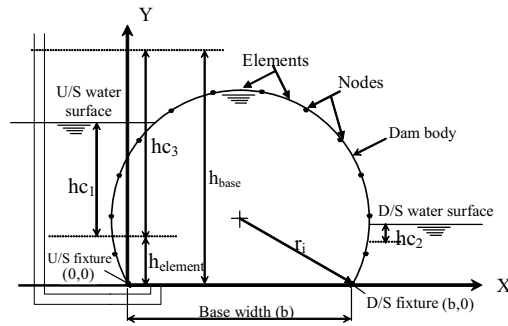


Figure 2. Division of the dam membrane length into (n) elements

and the results of these are the tension on the nodes.

Forces acting on an element can be described by the following equations:

$$F_u = \gamma \cdot hc_1 \cdot L \quad (1)$$

where,  $F_u$  is the upstream hydrostatic force on the element per unit length,  $\gamma$  the specific weight of the water,  $hc_1$  the vertical distance between upstream water surface and the centroid of the submerged length of element (Figure 2), and  $L$  is the length of the element.

$$F_{wa} = \gamma \cdot hc_3 \cdot L \quad (2)$$

where,  $F_{wa}$  is the internal water force on the element per unit length ( $F_{wa}$  equal to zero if air-inflated dam),  $hc_3$  is the vertical distance between the free water surface of the water pressure inside the inflatable dam and the centroid of the submerged length of element ( $h_{base} - h_{element}$ ) as shown in Figure 2.

$$F_a = p_{ia} \cdot L \quad (3)$$

where,  $F_a$  is the internal air force on the element per unit length ( $F_a$  equal to zero if water-inflated dam), and  $p_{ia}$  is the internal air pressure of the dam.

$$F_w = w \cdot L \quad (4)$$

where,  $F_w$  is the element weight per unit length, and  $w$  is the element weight per unit area.

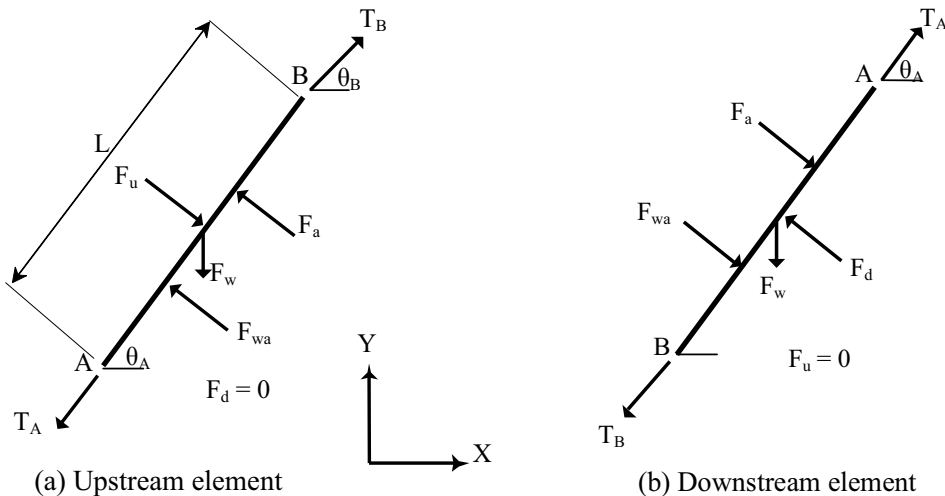


Figure 3. Forces acting on an element

Knowing the properties of the inflating fluid, and the membrane material of the inflatable dam, the forces on the element can be calculated using equations (1) to (4). Applying the principle of equilibrium for element AB (Figure 3) in horizontal and vertical directions we get:

$$\Sigma F_x: T_B \cdot \cos\theta_B = T_A \cdot \cos\theta_A + (F_a + F_{wa} - F_u) \cdot \sin\theta_A \quad (5)$$

$$\Sigma F_y: T_B \cdot \sin\theta_B = T_A \cdot \sin\theta_A + F_w + (F_u - F_a - F_{wa}) \cdot \cos\theta_A \quad (6)$$

where,  $T_A$  is the tension at node A per unit length,  $\theta_A$  the slope of element AB at node A,  $T_B$  the tension at node B per unit length, and  $\theta_B$  is the slope of element AB at node B.

To find the values of  $T_B$  and  $\theta_B$  for the element at node B it is necessary to assume trial values for  $T_A$  and  $\theta_A$  for the first element at node A. For the first element, after the values of  $T_B$  and  $\theta_B$  are determined, it will be used as  $T_A$  and  $\theta_A$  for the next element. This procedure will continue until tension force and coordinates for last element's node are determined. In the case that the predicted coordinates of the last element's node obtained from the above procedure do not coincide with its actual fixed location at the canal bed, then the Newton-Raphson method of iteration is applied in order to improve the initial trial values of  $T_A$  and  $\theta_A$  for the first element at node A to reduce the error in the coordinate of the last element's node.

For the downstream element the value of the force  $F_u$  is equal to zero, and the effect of the downstream water head  $F_d$  must be considered in the analysis.

$$F_d = \gamma \cdot hc_2 \cdot L \quad (7)$$

where,  $F_d$  is the downstream hydrostatic force on the element per unit length, and  $hc_2$  the vertical distance between the downstream water surface and the centroid of the submerged length of element (Figure 2). It should be noted that both forces  $F_u$  and  $F_d$  cannot act on the same element of the inflatable dam.

### Initial Values of Tension and Slope

To obtain the initial trial value of tension

$T_A$  for the first upstream element, the following expression is used assuming the shape of the membrane to be circular as taken by Parbery (1976):

$$T_A = p_i \cdot r_i \quad (8)$$

where,  $T_A$  is the maximum tension force of the membrane material per unit length,  $p_i$  the internal pressure, and  $r_i$  is the initial radius of curvature of the circular inflatable dam (Figure 2).

Assuming the downstream slope of the inflatable dam is zero, and the tension along the membrane is constant, the horizontal equilibrium of static forces acting on the inflatable dam (Figure 1(a)) is:

$$\frac{1}{2} \cdot \gamma \cdot (H_u)^2 = T_A + T_A \cdot \cos\theta_A + \frac{1}{2} \cdot \gamma \cdot (H_d)^2 \quad (9)$$

Then

$$\theta_A = \cos^{-1} \left\{ \left[ \frac{\gamma}{2} \cdot (H_u^2 - H_d^2) \right] / T_A - 1 \right\} \quad (10)$$

where,  $\theta_A$  is the slope of the inflatable dam at upstream fixture,  $H_u$  the upstream water head, and  $H_d$  is the downstream water head.

### Co-ordinate of Element Nodes of the Dam Profile

From the analysis of the hydrostatic forces on the element, the magnitude and direction of the tension force in each element can be determined. When the initial trial values of the tension and slope of the first element are calculated from equations (8) and (10) and by knowing the co-ordinates of the first node (upstream fixture (0,0)), the co-ordinates of the second node can be calculated using the angle and length of the element after elongation due to the tension. And by considering the hydrostatic forces applied on the first element, the value of the tension and slope in the next node can be calculated from equations (5) and (6). The procedure is repeated for all elements to calculate the co-ordinates of each node and therefore the cross-section of the inflatable dam. The details of this procedure are explained below:

- i) Divide the length of the membrane into n number of equal elements, (Figure 4(a)).
- ii) Calculate the initial values of tension and slope for the first element, (Figure 4(b)).
- iii) Calculate the elongation  $\Delta L$  of the element by using the stress-strain relationship of the model membrane material, (Figure 4(c)); the stresses can be calculated from the following expression:
- iv) Knowing the initial slope and new length  $L+\Delta L$  of the first element, and the co-ordinates of the first node (x (i), y (i)) assumed (0,0), the co-ordinates of the second node (x (i+1), y (i+1)) can be found (Figure 4(d)) from the following equations:

$$\sigma = \frac{T}{t} \tag{11}$$

where,  $\sigma$  is the stress in the membrane material, T the tension of the membrane material per unit length, and t is the thickness of the membrane material.

$$X (i+1) = (L + \Delta L) \cdot \text{Cos}\theta_A \tag{12}$$

$$Y (i+1) = (L + \Delta L) \cdot \text{Sin}\theta_A \tag{13}$$

The forces acting on the first element can be computed from equations (1), (2), (3) and (4).

The horizontal and vertical components of the tension at the second node can be calculated from equations (5) and (6), the magnitude and direction of the combined tension at the second element are found. The co-ordinates of the third node can be found by repeating steps 3 and 4.

In general the calculated co-ordinates of the last node do not coincide with the known co-ordinates (downstream fixture). The closing error results from the initial trial values of tension and slope of the first element and it is necessary to improve these values and the procedure is repeated from step 3 until the calculated co-ordinates of the last node coincide with the downstream fixture.

### Improving Initial Values for Tension and Slope

In the case that the trial values of the initial tension  $T_A$  and slope  $\theta_A$  of the first element result in the coordinates of the last node of the cross-section of inflatable dam not matching with the downstream fixture, it is necessary to improve these trial values. The Newton-Raphson iteration method of two simultaneous non-linear equations with two unknowns is used to improve the initial trial values of tension and slope. It is not possible to describe the cross-section of the inflatable dam using appropriate equations, which are convenient for differentiation. So, the differential coefficients of these equations can be determined

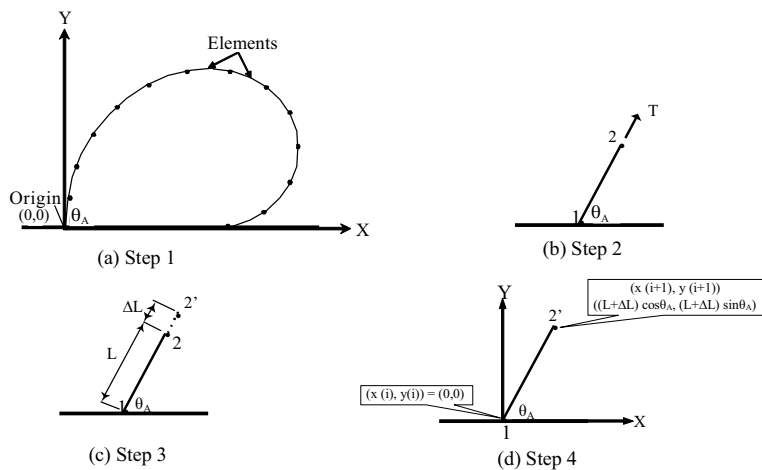


Figure 4. Co-ordinates of nodes of the dam profile

approximately by numerical means as proposed by Harrison (1970). The improved values of  $T_A$  and  $\theta_A$  are determined numerically from Newton's expressions:

$$T_{Ai} = T_A - (x * \delta y / \delta \theta_A - y * \delta x / \delta \theta_A) / z \quad (14)$$

$$\theta_{Ai} = \theta_A - (y * \delta x / \delta T_A - x * \delta y / \delta T_A) / z \quad (15)$$

where,  $T_{Ai}$  is the improved value of  $T_A$ ,  $\theta_{Ai}$  the improved value of  $\theta_A$ , and  $z$  is  $(\delta x / \delta T_A * \delta y / \delta \theta_A) - (\delta y / \delta T_A * \delta x / \delta \theta_A)$

The adjustment procedure of the tension and slope of the first element is illustrated in Figure 5. When the dam is analyzed under a guessed pair of values of initial tension  $T_A$  and slope  $\theta_A$  in the first upstream element, there will be a misclose at the downstream fixture, which can be represented by the error components  $x$  and  $y$  (Figure 5(a)). When the analysis is repeated with first the assumed tension increased by a small amount  $\delta T_A$ , and then the angle slope increased by a small amount  $\delta \theta_A$ , different misclose components will be calculated from which the rate of change of the  $x$  misclose and  $y$  misclose with respect to  $T_A$  and  $\theta_A$  can be

calculated as shown in Figures 5(b) and (c) respectively.

The procedure of improving  $T_A$  and  $\theta_A$  is repeated until the calculated miscloses  $x$  and  $y$  are reduced to negligible values which are within predetermined limits.

It is worth mentioning that another method was used in the computer program to improve initial values of tension and slope of the first element by using two loops, one loop (inner loop) for changing the values of initial tension and the other loop (outer loop) for changing the values of initial slope. Such a method was used in the situation when no convergence of solutions occurred by using the Newton-Raphson method.

Figure 6 shows the flow chart of this program. The program is able to analyze the dam when inflated by air, water and both air and water. The input data are:

- i) Properties of membrane material (density, thickness, polynomial coefficients of stress-strain relationship).
- ii) Membrane perimeter length.
- iii) Number of elements.
- iv) Upstream and downstream water head.

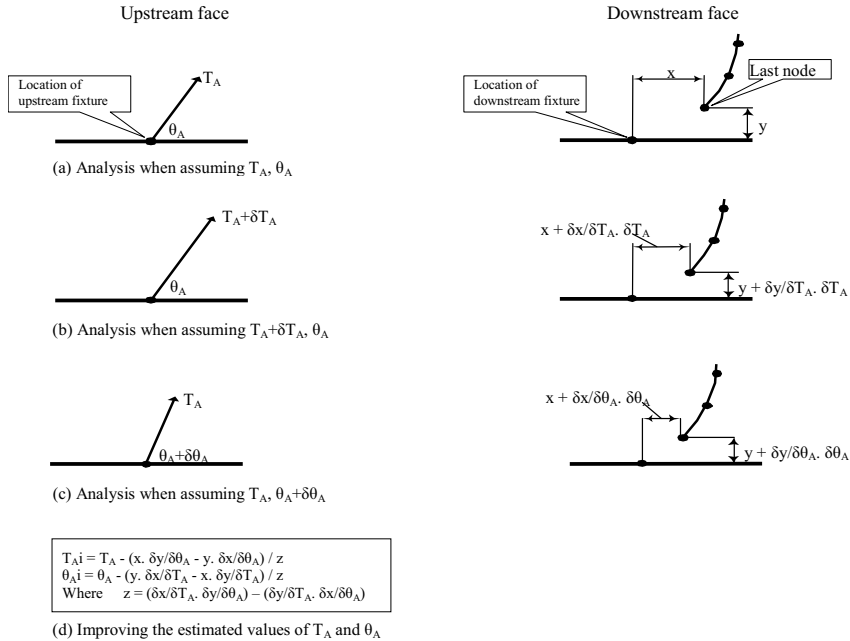


**Figure 5. Improving initial  $T_A$  and  $\theta_A$  to reduce the miscloses**

- v) Air pressure and water pressure head.
- vi) Co-ordinates of first and last node.
- vii)  $x$  and  $y$  misclose tolerance of last node.

When the theoretical analysis has been completed, the output results are:

- i)  $x$  and  $y$  co-ordinates of each node.
- ii) Tension and slope of each element.
- iii) All the forces acting on each element ( $F_u, F_a, F_{wa}, F_w, F_d$ ).
- iv) Cross-sectional area of the dam.
- v) New length of the membrane (stretched length).
- vi) Dam height.
- vii)  $x$  and  $y$  misclose values.
- viii) Plot of the cross-section of the dam.

The program will also plot the cross-section of the dam and calculate the cross-sectional area for the experimental data on the

air and water inflated dams under hydrostatic conditions, which are to be compared with those results obtained from the theoretical analysis.

### Materials and Methods

In this study the properties of the model membrane such as density, thickness, and stress-strain relationship were measured in the laboratory. The properties of the dam membrane material used for the inflatable dam model are thickness 1 mm, weight 1.3 kg/m<sup>2</sup>, and the tensile strength 6.45 kN/m<sup>2</sup>.

The procedure given by ASTM D412 (1985) was followed to determine the tensile stress for rubber material. The relationship between the stress and the strain of rubber material is shown in Figure 7. It could be seen

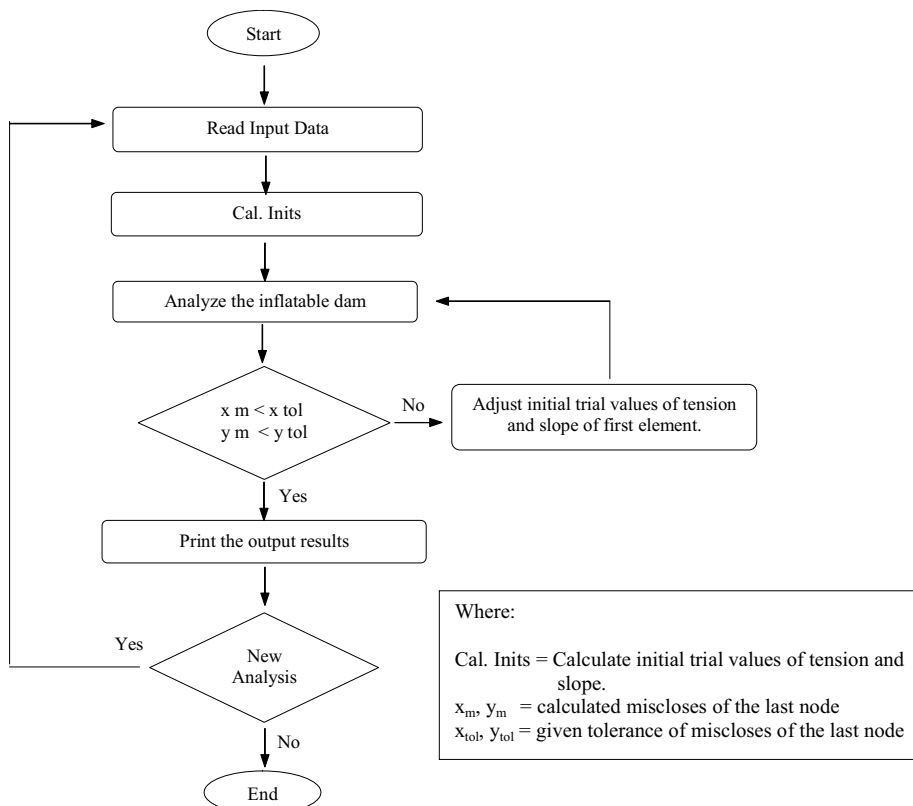
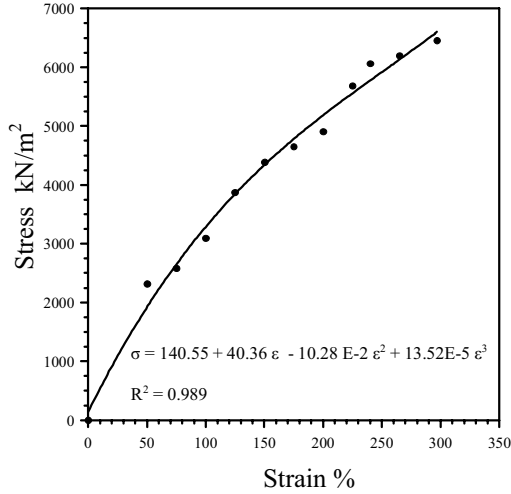


Figure 6. Flow chart of the computer program



**Figure 7. Stress-strain relationship of the dam model membrane material**



**Figure 8. Dam model and the flume**

that the relationship is nonlinear. The equation for best fitting curve was found to be a polynomial of 3<sup>rd</sup> degree given by the following general form equation:

$$\sigma = C_1 + C_2 \varepsilon + C_3 \varepsilon^2 + C_4 \varepsilon^3 \quad (16)$$

where,  $\varepsilon$  is the strain in the element of the membrane material =  $\Delta L/L\%$ ,  $\sigma$  the stress in the element of the membrane material,  $\Delta L$  the elongation in the element of the membrane material,  $L$  the original length of the element of the membrane material, and  $C_1, C_2, C_3, C_4$  are the polynomial coefficients and their values are

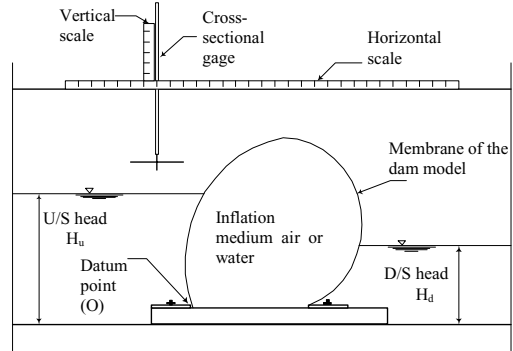


**Figure 9. Cross-sectional gage**

140.55, 40.36, -10.28E-2 and 13.52E-5 respectively.

The experiments were performed using a rectangular glass-sided walled flume having a length of 20 m, width of 0.9 m and depth of 0.6 m. Water level and dam cross-section displacement, horizontally and vertically, were recorded using a cross-sectional gage (Figures 8 and 9).

Air pressure inside the dam model was measured with a water manometer tube. An air compressor was used to inflate the dam model. A steel column of external diameter of 200 mm was used to inject water into the dam model. A piezometer was connected to the steel column to measure the water pressure inside the model. A rubber material was used to build the air and water inflated dam models, which, made from a rectangular rubber sheet with the perimeter length of 0.55 m, membrane thickness of 0.001 m and base length of 0.15 m, have been employed and anchored to the model base which is linked tightly to the flume bed as shown in Figure 10 (Alhamati, 2002).

## Results and Discussion

### Comparison Between Experimental and Theoretical Results

The crest height and cross-sectional area at the center of the dam model were recorded in the laboratory. The cross-sectional area for the dam model was computed by recording the coordinates of the dam profile, and Simpson's

rule was applied to compute the values of the cross-sectional area. These values were compared with those obtained from the theoretical analysis. Tables 1 and 2 show this comparison. The number of elements  $n$ , used in the theoretical analysis was 300 elements. This number was selected after many trials and it was found that any increment of the elements (beyond 300) did not change the results obtained from the analysis significantly. It was found that theoretical and experimental values for the dam height and dam

cross-sectional area in a good agreement. The comparison between the predicted and measured dam cross-section of some cases are given in Figures 11 and 12. Good agreements between observed and predicted profiles for the inflatable dam were obtained at high pressure inside the inflatable dam model (Figures 11(a) and 12(a)). It is observed that at low pressure inside the inflatable dam model, a difference between the observed and predicted profiles of the inflatable dam was obtained (Figures 11(b) and 12(b)). This

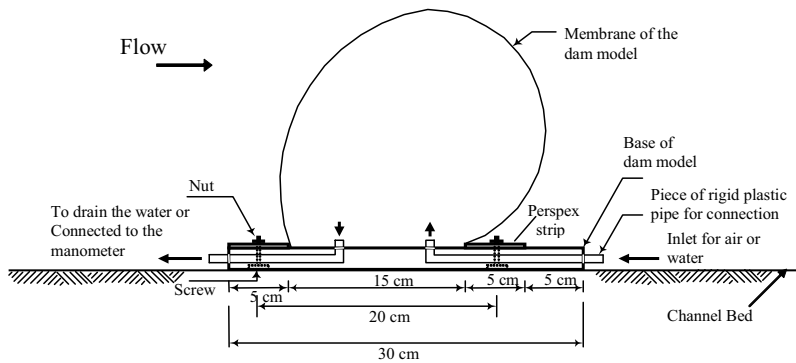


Figure 10. Anchoring the inflatable dam model to the model base

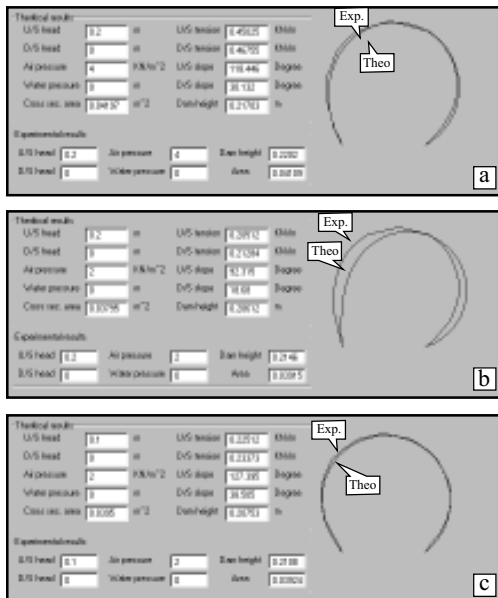


Figure 11. Experimental and theoretical cross-section of air-inflated dam

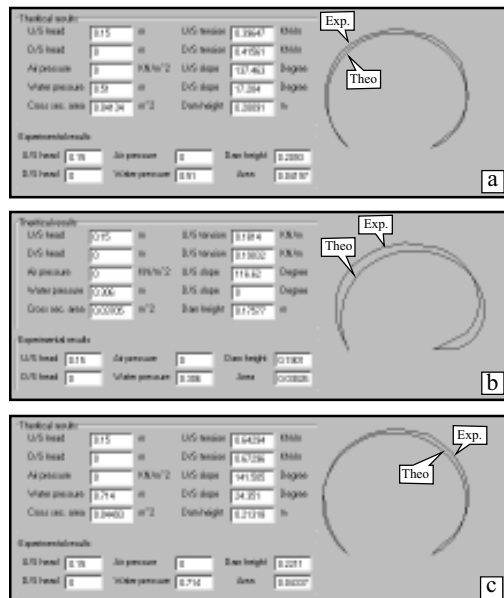


Figure 12. Experimental and theoretical cross-section of water-inflated dam

**Table 1. Comparison between theoretical and experimental dam height and cross-sectional area (Air-inflated dams - hydrostatic conditions)**

Test no.	Inside air pressure (kN/m <sup>2</sup> )	U/S head (mm)	D/S head (mm)	Dam height (mm)		% Abs. Diff. in height	Cross-sectional area (mm <sup>2</sup> )		% Abs. Diff. in area
				Exp.	Threo.		Exp.	Threo.	
1		50	0	205.60	204.09	0.73	38,000	38,890	2.34
2		100	0	208.00	205.67	1.12	38,100	38,720	1.63
3		150	0	211.90	207.40	2.12	36,600	38,250	4.51
4	1.5		0	212.60	194.26	8.63	38,000	35,250	7.24
5		200	50	213.60	201.01	5.89	37,800	35,970	4.84
6			100	216.20	209.50	3.10	37,900	36,410	3.93
7			150	221.80	218.92	1.29	37,460	36,670	2.10
8		50	0	209.00	206.00	1.44	39,700	39,600	0.25
9	2	100	0	210.80	207.50	1.57	39,200	39,500	0.77
10		150	0	213.40	209.40	1.87	38,900	39,200	0.77
11		200	0	214.60	206.10	3.96	39,100	38,000	2.81
12		50	0	213.60	210.10	1.63	39,500	41,140	4.15
13	3	100	0	214.60	211.38	1.50	38,950	40,850	4.87
14		150	0	216.40	212.30	1.89	41,070	40,710	0.88
15		200	0	218.00	212.10	2.71	40,720	40,220	1.23
16		50	0	216.90	214.33	1.18	40,330	42,600	5.63
17	4	100	0	217.60	215.00	1.19	39,020	42,410	8.68
18		150	0	219.30	216.12	1.45	39,880	42,320	6.12
19		200	0	220.20	217.00	1.45	41,100	42,000	2.19
20		50	0	222.20	219.35	1.28	41,670	44,170	6.00
21		100	0	223.00	219.72	1.47	42,410	44,030	3.82
22		150	0	224.30	220.92	1.50	40,910	44,000	7.55
23	5		0	225.70	221.20	1.99	41,850	43,640	4.28
24		200	50	225.80	221.40	1.95	42,410	43,740	3.14
25			100	226.80	222.60	1.85	42,100	43,630	3.63
26			150	228.20	224.50	1.62	41,220	43,770	6.19
		Mean				2.17			3.82

is attributed to the effect of friction forces, which are developed between the right and left ends of the dam model and the channel walls. These forces had a significant effect on the dam displacement at low internal pressure.

Further analysis was carried out using the theoretical computation to investigate the behavior of inflatable dams under different conditions of internal pressure and upstream water head for both air and water-inflated dams under hydrostatic conditions. The effect of base length, membrane thickness, and membrane

perimeter length on the behavior of inflatable dams is also included in this study.

#### **Effect of Increasing Internal Pressure on the Cross-section and Height of the Dam Model**

Figures 13 and 14 show the effect of increasing internal pressure on the shape of the cross-sectional of an air-inflated dam and water-inflated dam respectively. The internal air pressure was changed from 1.5 kN/m<sup>2</sup> to 5 kN/m<sup>2</sup> with constant upstream head of 200 mm and downstream head equal to zero. Due to this

**Table 2. Comparison between theoretical and experimental dam height and cross-sectional area (Water-inflated dams - hydrostatic conditions)**

Test no.	Water pressure at dam base (kN/m <sup>2</sup> )	U/S head (mm)	D/S head (mm)	Dam height (mm)		% Abs. Diff. in height	Cross-sectional area (mm <sup>2</sup> )		% Abs. Diff. in area
				Exp.	Threo.		Exp.	Threo.	
1		50	0	186.90	177.90	4.82	37,040	38,140	2.97
2		100	0	188.00	177.50	5.58	37,210	37,530	0.86
3	3 kN/m <sup>2</sup> (306)	150	0	190.10	175.80	7.52	38,260	37,050	3.16
4			0	191.80	172.91	9.85	39,800	36,270	8.87
5		170	50	192.00	173.10	9.84	39,180	36,300	7.35
6			100	194.00	184.80	4.74	39,280	37,650	4.15
7			150	198.40	194.20	2.12	38,680	38,820	0.36
8		50	0	198.90	191.00	3.97	39,320	39,930	1.55
9	4 kN/m <sup>2</sup> (408)	100	0	199.70	192.10	3.81	39,440	39,860	1.06
10			150	0	201.60	192.00	4.76	40,790	39,830
11		170	0	202.30	189.60	6.28	39,330	39,150	0.46
12		50	0	206.90	199.10	3.77	42,540	41,650	2.09
13		100	0	207.70	199.80	3.80	42,730	41,570	2.71
14		150	0	209.30	200.90	4.01	41,970	41,340	1.50
15	5 kN/m <sup>2</sup> (510)	170	0	209.40	200.50	4.25	43,310	41,270	4.71
16			50	209.70	201.30	4.01	43,310	41,140	5.01
17		100	100	211.00	203.70	3.46	40,450	41,360	2.25
18		150	150	213.50	206.10	3.47	42,280	41,400	2.08
19		170	170	214.60	206.50	3.77	41,900	41,480	1.00
20		50	0	213.50	205.70	3.65	42,000	43,150	2.74
21	6 kN/m <sup>2</sup> (612)	100	0	214.10	206.30	3.64	42,070	42,960	2.12
22			150	0	215.40	207.60	3.62	43,210	43,040
23		170	0	215.90	207.10	4.08	44,460	42,920	3.46
24		50	0	219.10	211.70	3.38	44,720	44,940	0.49
25	7 kN/m <sup>2</sup> (714)	100	0	219.80	212.90	3.14	44,660	44,930	0.60
26			150	0	221.10	213.20	3.57	43,370	44,930
27		170	0	221.50	213.70	3.52	43,370	44,670	3.00
Mean						4.53			2.63

change, the resulting dam cross-section was changed to approximately a circular shape. This is also observed for a water inflatable dam when the internal water pressure head was changed from 3 kN/m<sup>2</sup> (306 mm) to 7 kN/m<sup>2</sup> (714 mm) at dam base. In both cases large deformation occurred with low internal pressures.

Figure 15 shows the effect of internal pressure on the dam height. It was observed that the dam height increases significantly with the increase of the internal pressure. This can be used to adjust the dam height in order to control

water depth in the irrigation channels particularly when big discharges are needed.

#### **Effect of Increasing Upstream Water Head and Internal Pressure**

The effect of increasing the upstream water head and internal pressure on the behavior of inflatable dams was investigated through the tension in the membrane, dam height, upstream membrane slope (at upstream fixture), and elongation in the membrane.

The average tension between the upstream

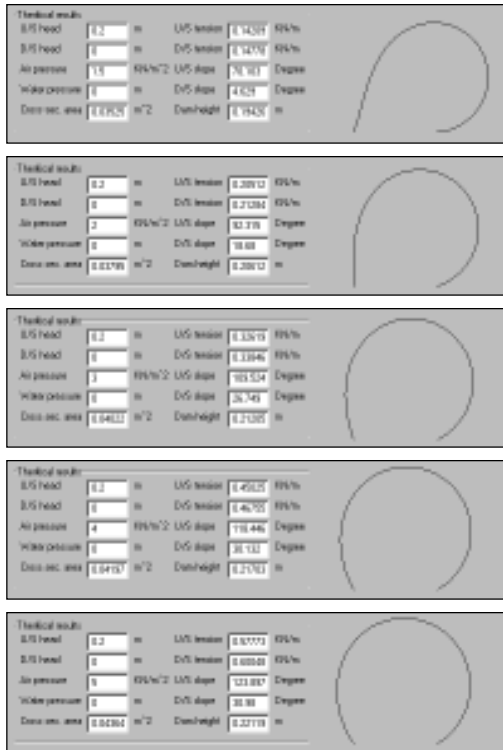


**Figure13. Effect of increasing internal pressure on the behavior of air-inflated dams for constant upstream and downstream water head**

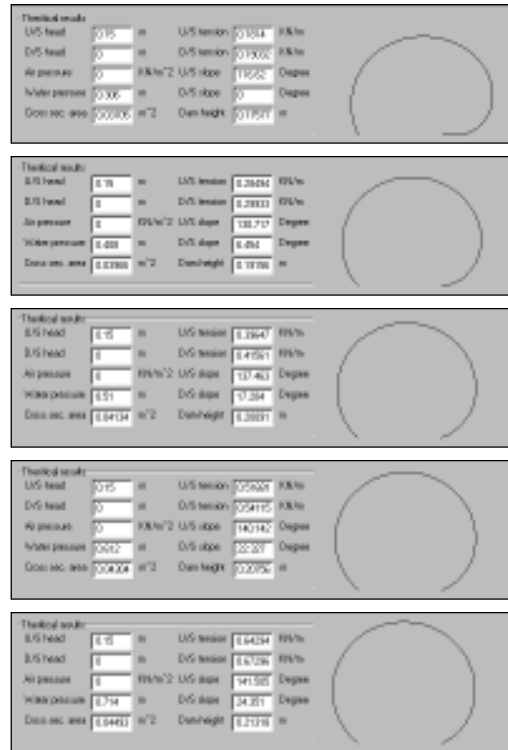
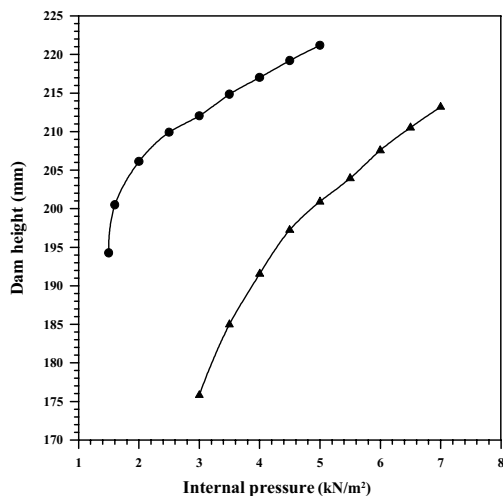


**Figure 14. Effect of increasing internal pressure on the behavior of water-inflated dams for constant upstream and downstream water head**

fixture and downstream fixture has been computed. Figure 16 shows that the tension in the membrane decreases with increasing the upstream head. Also the tension increased when the internal pressure increased. In Figure 16 with internal air pressure of 5 kN/m<sup>2</sup>, when the upstream water depth increased from 50 mm to 210 mm the tension through the dam membrane decreased from 0.61 kN/m<sup>2</sup> to 0.56 kN/m<sup>2</sup>. It is observed that the tension in the membrane was less for a water inflated dam than an air inflated dam under the same conditions of internal pressure and upstream water head. For example if a pressure of 4 kN/m<sup>2</sup> (408 mm) as internal pressure and an upstream water head of 100 mm are used, the resulted tensions were found to be 0.48 kN/m<sup>2</sup> and 0.3 kN/m<sup>2</sup> for an air inflated dam and a water inflated dam respectively (Figure 16).

Figure 17 shows that the height of the air-inflated dam increases with increasing upstream head, for all inside pressures. This behavior may not be true for all values of the internal pressure. For example, when the internal air pressure increased to 5 kN/m<sup>2</sup> and the upstream head was 200 mm the dam height reached a peak value of 221.98 mm and decreased to 221.03 mm when the upstream head was increased to 220 mm. Figure 17 shows also the variation of dam height with increasing upstream head for a water-inflated dam. Similar to the air-inflated dam at low water pressure 3 kN/m<sup>2</sup> (306 mm) the dam height decreases as the upstream head increases. The dam height rises slightly when the upstream head increases until the dam height reaches a peak value and then it falls slightly when the upstream head



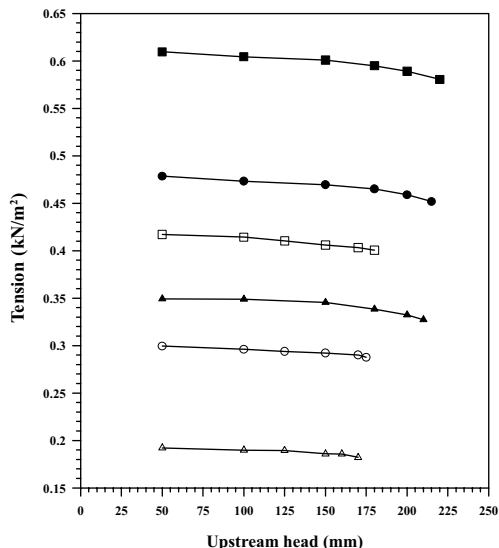
Type of dam	U/S water head (mm)	D/S water head (mm)	Symbol
Air-inflated	200	0	●
Water-inflated	170	0	▲

**Figure 15. Variation of dam height with increasing internal pressure for constant upstream and downstream water head**

increases (water pressure 3 kN/m<sup>2</sup> (408 mm) and 3 kN/m<sup>2</sup> (510 mm))

Figure 18 shows the variation of the upstream slope (slope at upstream fixture) with increasing the upstream water head and internal pressure for air and water-inflated dams. The upstream slope decreases with increasing the upstream head, which indicates a deformation towards the downstream side. The rate of decrease in the upstream slope is greater for low internal pressure (3 kN/m<sup>2</sup>) than high internal pressure (5 kN/m<sup>2</sup>). The same behavior was found in water-inflated dams but the upstream slope is higher for low water pressure than the upstream slope of high water pressure with low upstream head. But when increasing the upstream head the upstream slope for high water pressure is greater than those for low water pressure. This may be due to the fact that the dam begins to flatten at the upstream fixture when the internal pressure and upstream head are decreasing.

The stretch in the membrane's original length has been noticed, and this occurs due to



Type of dam	Internal pressure (kN/m <sup>2</sup> )	Symbol
Air-inflated	3	▲
	4	■
	5	□
Water-inflated	3	△
	4	○
	5	□

D/S water head equal to zero.

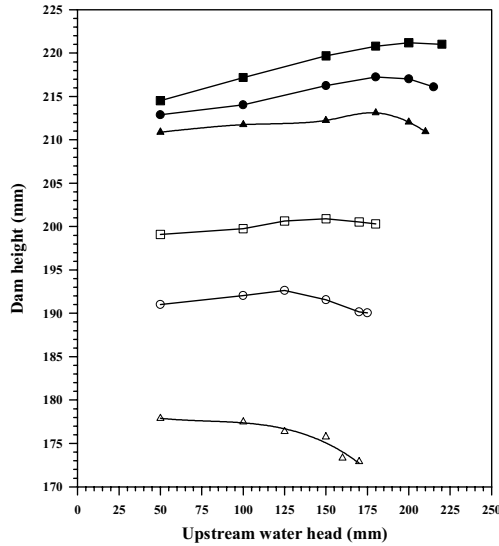
**Figure 16. Variation of membrane tension with rising upstream water head for various internal pressures**

the applied loads (upstream water head, downstream water head and internal pressure) and can be found from the stress-strain relationship.

The elongation of the membrane material was found by subtracting the original length from the new length (stretched length). Figure 19 shows that the elongation increases when the internal pressure increases or when the upstream head decreases. It is well known also that the elongation in membrane material is directly affected by the material properties of the membrane.

**Effect of Increasing the Perimeter Length, Thickness and Base Length of the Dam Model on the Membrane Tension and Dam Height**

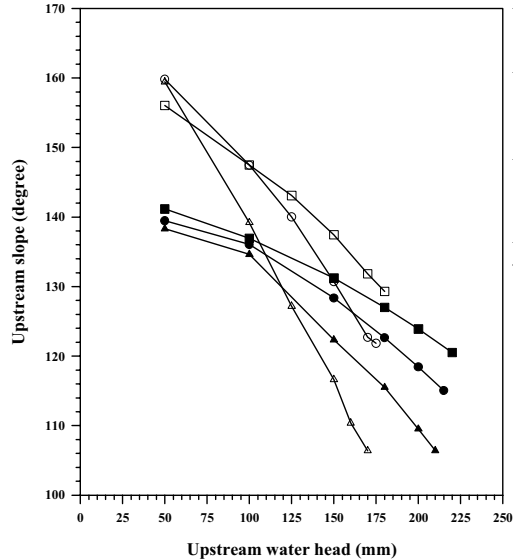
The membrane tension and dam height were investigated by increasing the membrane perimeter length from 450 mm to 650 mm for both air and water inflated dams. Figure 20 shows



Type of dam	Internal pressure (kN/m <sup>2</sup> )	Symbol
Air-inflated	3	▲
	4	▼
	5	■
Water-inflated	3	△
	4	□
	5	▢

D/S water head equal to zero.

**Figure 17. Variation of dam height with rising upstream water head for various internal pressures**



Type of dam	Internal pressure (kN/m <sup>2</sup> )	Symbol
Air-inflated	3	▲
	4	▼
	5	■
Water-inflated	3	△
	4	□
	5	▢

D/S water head equal to zero.

**Figure 18. Variation of membrane slope at upstream fixture for rising upstream water head and various internal pressures**

that increasing the membrane perimeter length for an air-inflated dam results in an increase in the membrane tension. Also the height of the dam increases when increasing the membrane perimeter length (Figure 21).

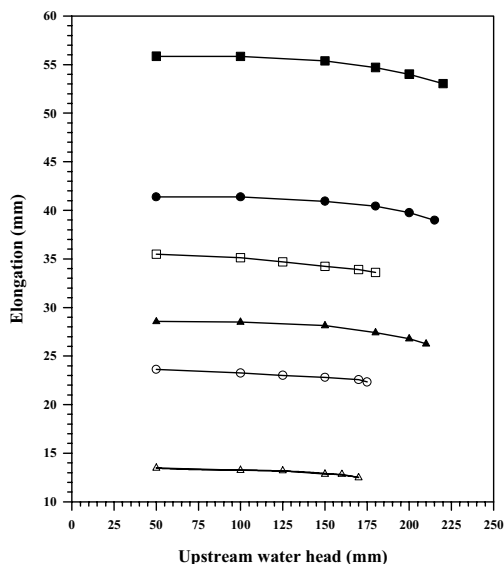
The same behavior was found in the case of a water-inflated dam (Figures 20 and 21) but with a low rate of increase in tension and height compared with an air-inflated dam.

The effect of variation in membrane thickness on the tension and the dam height was investigated by using a membrane thickness that varies from 0.5 mm to 3.5 mm. Figures 22 and 23 show the behavior of an air-inflated dam with increasing the membrane thickness. Increasing the membrane thickness produces a decrease in tension of the membrane. Also the height of the dam decreases when the membrane thickness increases.

The behavior of a water-inflated dam when increasing the membrane thickness is the same as an air-inflated dam, but the rate of decrease is lower than that in the latter (Figures 22 and 23).

The effect of variation in the base length of the dam (distance between upstream and downstream anchor) on the tension in the membrane and dam height was investigated for both air and water inflated dams by increasing base length from 120 mm to 250 mm. The results of these tests are shown in Figures 24 and 25.

For an air-inflated dam, as the base length increases the membrane tension also increases (Figure 24). The dam height also increases with the base length reaching its peak value at 219.22 mm with internal air pressure equal to 4 kN/m<sup>2</sup>; however, further increase in the base length beyond 220 mm causes the dam height to start decreasing (Figure 25).



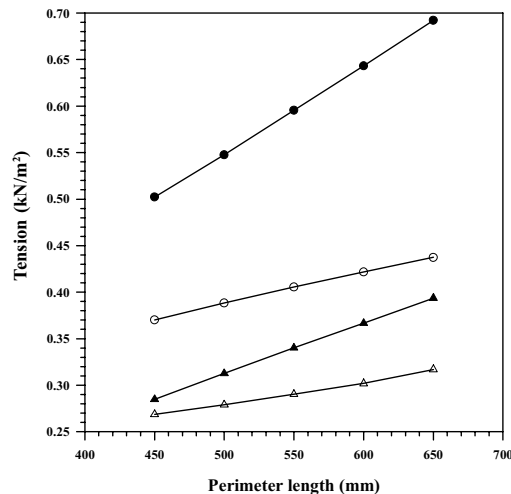
Type of dam	Internal pressure (kN/m <sup>2</sup> )	Symbol
Air-inflated	3	▲
	4	▼
	5	◆
Water-inflated	3	△
	4	○
	5	□

D/S water head equal to zero.

**Figure 19. Variation of elongation in membrane for rising upstream water head and various internal pressures**

In the case of a water-inflated dam the same behavior is found as in an air-inflated dam. That is, increasing the base length causes an increase in tension in the membrane. However, the peak value of the dam height of 197.15 mm occurs at a base length of 220 mm; beyond this value the height of the dam starts to decrease in reverse trend (internal water pressure equal to 4 kN/m<sup>2</sup> (408 mm) (Figures 24 and 25).

The dimensions of the model used for the inflatable dam were not based on the dimensions of a specific existing prototype but a reasonable scale is used to assume the dimension of model considering the available space in the laboratory to conduct the experiments. The concept of similarity between the model and the prototype should be applied to make use of the results obtained but the material of membrane of the model and that of the prototype must have



Type of dam	Internal pressure (kN/m <sup>2</sup> )	U/S water head (mm)	Symbol
Air-inflated	3	170	▲
	5	170	◆
Water-inflated	4	150	△
	5	150	○

Membrane thickness = 1 mm.  
Base length = 150 mm.  
D/S water head equal to zero.

**Figure 20. Variation of membrane tension with membrane perimeter length**

similar properties. Also, the relationship of the internal pressure between the model and prototype should be considered.

### Conclusion

Physical models were employed to study the behavior of the inflatable dams under hydrostatic conditions. The shape, dam height and cross-sectional area, which were obtained from the theoretical analysis, were compared with those obtained from the experimental work. In general, a good agreement was found between the experimental measurements and the results of theoretical analysis obtained from the computer program. From the present study the following conclusions can be made:

- i) The inflatable dam becomes rigid when inflated to high pressures, which results in insignificant deformation in shape when the upstream head is changed.

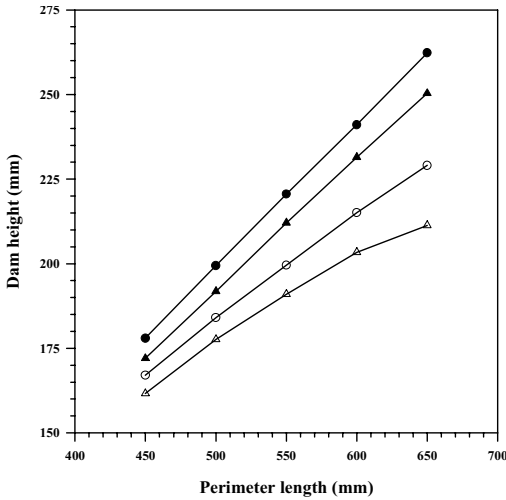


Figure 21. Variation of dam height with membrane perimeter length

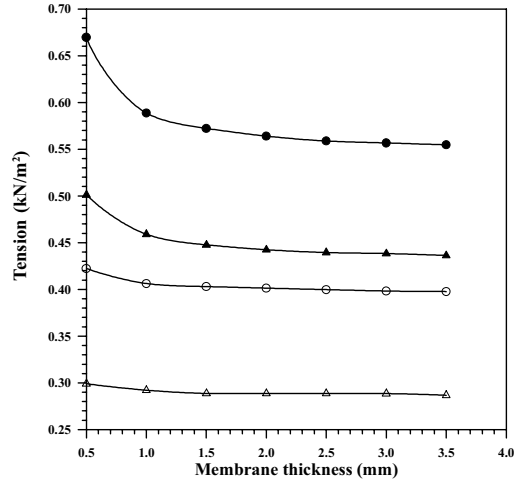


Figure 22. Variation of membrane tension with membrane thickness

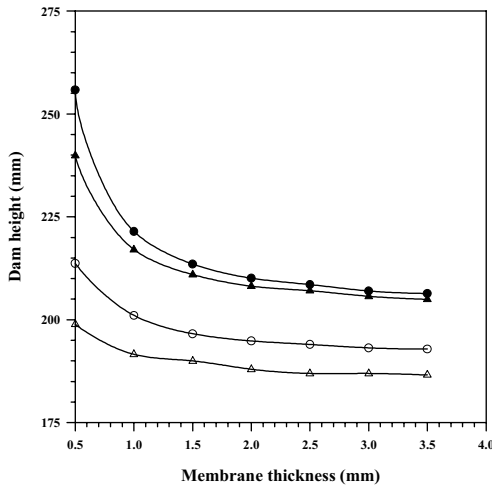


Figure 23. Variation of dam height with membrane thickness

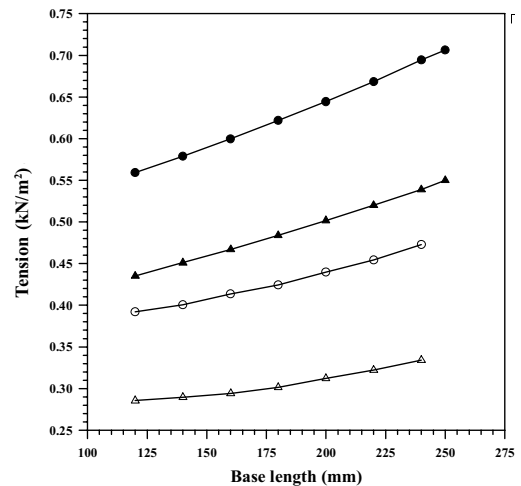
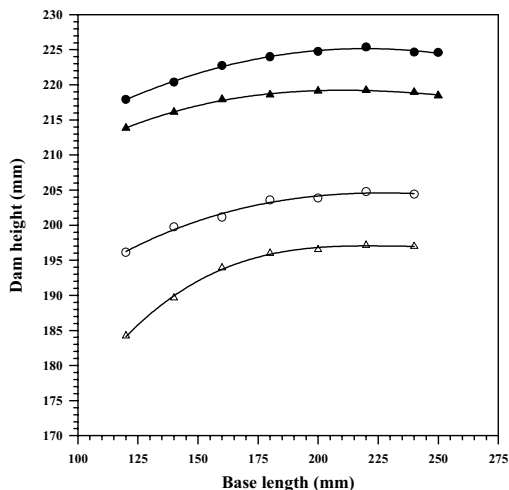


Figure 24. Variation of membrane tension with dam base length



Type of dam	Internal pressure (kN/m <sup>2</sup> )	U/S water head (mm)	Symbol
Air-inflated	4	200	●
	5	200	▲
Water-inflated	4	150	○
	5	150	△

Membrane perimeter length = 553 mm.  
 Membrane thickness = 1 mm.  
 D/S water head equal to zero.

**Figure 25. Variation of dam height with dam base length**

- ii) Dam height of an air-inflated dam was higher than that for a water-inflated dam at the same conditions of internal pressure and upstream and downstream water head, which means that an air-inflated dam can support a higher upstream water head than a water inflated dam.
- iii) It is found that increasing the upstream water head of an air-inflated dam from 50 mm to 175 mm with the internal pressure 4 kN/m<sup>2</sup> decreases the upstream slope by 16.9°. In comparison, with a water inflated-dam at the same conditions (408 mm internal pressure), the decrease in upstream slope is 37.98° when increasing the upstream head from 50 mm to 175 mm. This shows that the magnitude of deformation depends on the type of medium of inflation.

- iv) The stretch in the membrane of an air-inflated dam is higher than that of a water-inflated dam, which is due to the high tension in an air-inflated dam and this may cause a reduction in the dam life.
- v) The tension in the membrane and dam height increased with increasing the membrane perimeter length, and also the tension increased when increasing the base length.
- vi) Increasing the membrane thickness decreases the dam crest height. The dam crest height increases with increasing the dam base length up to a certain base length, then it starts to decrease with a further increase in the dam base length.
- vii) The convergence process was found to be critically dependent upon the choice of the initial values for the tension and slope in the first element (different values of initial tension and slope were used for different cases). In some situations no convergence occurred especially at low internal pressure. This creates a physical instability of the dam membrane because some elements of the membrane may not be subject to tension force and the theoretical analysis used is applicable for membrane elements under tension only.

**References**

Alhamati, A.A. (2002). Investigation and analysis of inflatable dams [M.Sc. thesis]. Building and Construction Department, University of Technology, Baghdad, Iraq, p. 117.

Al-Shami, A. (1983). Theory and design of inflatable structures [Ph.D. thesis]. University of Sheffield, Sheffield, United Kingdom, p. 185.

Alwan, A.D. (1979). The analysis and design of inflatable dams [Ph.D. thesis]. University of Sheffield, Sheffield, United Kingdom, p. 195.

- Anwar, H.O. (1967). Inflatable dams. *Journal of the Hydraulics Division, ASCE*, 93(Hy3): 99-119.
- Abd alsaber, I.B. (1997). Effects of sediments and tailwater depths on the performance of air inflated dams. [Ph.D. thesis]. University of Mosul, Mosul, Iraq, p. 95.
- Annual Book of ASTM Standards. (1985). Standard Test Methods for Rubber Properties in Tension, Vol. 08.01(D412).
- Binnie, G.M., Thomas, A.R, and Gwyther, J.R. (1973). Inflatable Weir Used During Construction of Mangala Dam. *Proceedings of the Institution of Civil Engineers; Part 1*, 54: 625-639.
- Dumont, U. (1989). The use of inflatable weirs for water level regulation. *International Water Power and Dam Construction*, 41(10):44-46.
- Harrison, H.B. (1970). The analysis and behavior of inflatable dams under static loading. *Proceedings of the Institution of Civil Engineers*, 45:661-676.
- Harrison, H.B. (1971). The analysis and behavior of inflatable dams under static loading (Discussion). *Proceedings of the Institution of Civil Engineers*, 48:131-139.
- Hsieh, J.C., Plaut, R.H., and Yucel, O. (1989). Vibrations of an inextensible cylindrical membrane inflated with liquid. *Journal of Fluids and Structures*, 3:151-163.
- Imbertson, N.M. (1960). Automatic rubber diversion dam in the Los Angeles River. *Journal of American Water Works Association*, 52:1,373-1,378.
- Nicholas, M.H. and Rangaswami, N. (1983). Flexible dams inflated by water. *Journal of Hydraulic Engineering, ASCE*, 109(7): 1,044-1,048.
- Parbery, R.D. (1976). A continuous method of analysis for the inflatable dam. *Proceedings of the Institution of Civil Engineers, Part 2*, 61:725-736.
- Parbery, R.D. (1978). Factors affecting the membrane dam inflated by air pressure. *Proceedings of the Institution of Civil Engineers, Part 2*, 65: 645-654.
- Plaut, R.H., and Fagan, T.D. (1988). Vibrations of an inextensible, air-inflated, cylindrical membrane. *Journal of Applied Mechanics*, 55: 672-675.
- Plaut, R.H., and Leeuwrik, J.M. (1988). Non-linear oscillations of an inextensible, air-inflated, cylindrical membrane. *International Journal of Non-Linear Mechanics*, 23(5/6):347-353.
- Takasaki, M. (1989). The omata inflatable weir, at the Kawabi hydro scheme, Japan. *International Water Power and Dam Construction*, 41(1):39-41.
- Tam, P.W.M. (1998). Use of inflatable dams as agricultural weirs in Hong Kong. *Journal of Hydraulic Engineering, ASCE*, 124(12): 1,215-1,226.
- Zhang, X.Q., Tam, P.W.M., and Zheng, W. (2002). Construction, operation, and maintenance of rubber dams. *Canadian Journal of Civil Engineering*, 29:409-420.